Agricultural and Forest Meteorology 152 (2012) 189–200

Contents lists available at SciVerse ScienceDirect

Agricultural and Forest Meteorology

journal homepage: www.elsevier.com/locate/agrformet

Ecological controls on net ecosystem productivity of a seasonally dry annual grassland under current and future climates: Modelling with *ecosys*

R.F. Grant[a,*], D.D. Baldocchi[b], S. Ma[b]

[a] *Department of Renewable Resources, University of Alberta, Edmonton, AB, Canada T6G 2E3*
[b] *Department of Environmental Science, Policy and Management & Berkeley Atmospheric Science Center, University of California, Berkeley, CA, United States*

ARTICLE INFO

Article history:
Received 14 January 2011
Received in revised form 26 August 2011
Accepted 10 September 2011

Keywords:
CO_2 fluxes
Net ecosystem productivity
Phenology
Seasonally dry grasslands
Climate change
Ecosys

ABSTRACT

Net ecosystem productivity (NEP) of seasonally dry grasslands in Mediterranean climate zones is determined by the duration and intensity of rainy *vs.* dry seasons. Precipitation in these zones is expected to decline with climate change during the next century, possibly reducing NEP. Ecosystem models used to study climate change impacts on grasslands in these zones need first to simulate effects of soil wetting and drying on the duration and intensity of net C uptake and emission during rainy and dry seasons under current climate. Continuous eddy covariance (EC) measurements of CO_2 and energy exchange provide well constrained tests of such models. In this study, hourly CO_2 and energy exchange from the ecosystem model *ecosys* were tested against EC measurements recorded over an annual grassland at Vaira Ranch, CA in a Mediterranean climate zone during eight years (2001–2008) with variable rainy seasons. Variation in measured CO_2 and latent heat fluxes was sufficiently well simulated during each year of the study ($0.7 < R^2 < 0.9$) that most of the variation unexplained by the model could be attributed to uncertainty in the measurements. Interannual variation in NEP from the model was also correlated with that from EC measurements ($R^2 = 0.75$). Annual NEP from both the model and EC were correlated with the duration of net C uptake, but not with the amount of precipitation, during the rainy seasons. Average annual NEP of the grassland modelled from 2001 to 2008 was 29 $\mathrm{g\,C\,m^{-2}\,y^{-1}}$ with an interannual variation of ±110 $\mathrm{g\,C\,m^{-2}\,y^{-1}}$ caused by that in the duration of net C uptake. During climate change (SRES A1fi and B1 under HadCM3), changes in modelled NEP were determined by changes in duration and intensity of net C uptake in rainy seasons *vs.* net C emission in dry seasons. In years with briefer rainy seasons, modelled NEP rose because rates of net C uptake increased with higher temperature and CO_2 concentration, while the duration of net C uptake remained limited by that of the rainy season. However in years with longer rainy seasons, modelled NEP declined because the duration of net C uptake was reduced when warming hastened phenological development and caused maturity of annual plants to be reached before the end of the rainy season. As climate change progressed, declines in annual NEP gradually exceeded rises, causing the small C sink modelled under current climate to be almost completely lost after 90 years under SRES A1fi (2 ± 103 $\mathrm{g\,C\,m^{-2}\,y^{-1}}$) and B1 ($6 \pm 95$ $\mathrm{g\,C\,m^{-2}\,y^{-1}}$).

1. Introduction

Seasonally dry annual grasslands are an important ecosystem type in Mediterranean climate zones. Those in California alone occupy more than 4.4 Mha or 20% of the area of the state (Huntsinger et al., 2007). Net ecosystem productivity (NEP) of these grasslands is thought to be determined by the duration and intensity of precipitation in the rainy season during which soils are wet enough to sustain net C uptake by plants (Ma et al., 2007). This net C uptake is offset by slow net C emission during the dry season when grasslands have senesced, by rapid, rainfall-induced pulses of net C emission at the start of the next rainy season before grasslands regrow, and sometimes by rapid net C emission at the end of the rainy season if grassland growth terminates before the start of the following dry season. At an annual time scale, net C uptake during the mid rainy season may or may not exceed net C emission during the dry season and during the start and end of the rainy season, so that these grasslands may be either sinks or sources of C.

These ecological controls on net C uptake *vs.* emission in seasonally dry grasslands have been demonstrated with eddy covariance (EC) measurements. Xu and Baldocchi (2004) attributed annual NEP of a northern California grassland to the timing of rain events that determined the duration of net C uptake in the rainy season, rather than to the total amount of rainfall received during the year. Ma et al. (2007) found that changes in the duration of net C uptake with precipitation caused this grassland to alternate between a sink

---

* Corresponding author. Tel.: +1 780 492 6609; fax: +1 780 492 1767.
E-mail address: robert.grant@ales.ualberta.ca (R.F. Grant).

0168-1923/$ – see front matter © 2011 Elsevier B.V. All rights reserved.
doi:10.1016/j.agrformet.2011.09.012

or source of C. Pereira et al. (2007) made a similar finding for a Mediterranean grassland in Portugal.

The climatic signals initiating and terminating net C uptake in seasonally dry grasslands are therefore important ecological controls on NEP. Botta et al. (2000) used an index derived from modelled relative soil water content (RSWC) to estimate leafout in tropical deciduous ecosystems. Jolly and Running (2004) used precipitation *vs*. potential evapotranspiration and soil water potential *vs*. net C uptake to estimate dates of leafout and leafoff respectively in drought deciduous ecosystems. However a definitive method has not yet been developed for estimating dates on which C uptake is initiated and terminated in seasonally dry grasslands. For annual grasslands, this method needs also to account for initiation and termination of net C uptake with seed germination and plant maturity.

Understanding the ecological controls on net C uptake *vs*. emission in seasonally dry grasslands is essential to reduce uncertainties in predicting climate change impacts on NEP. These impacts may be particularly adverse in Mediterranean climate zones because precipitation in these zones is generally expected to decline (Christensen et al., 2007). In model projections of climate change impacts in Europe, NEP in Mediterranean regions was expected to be adversely impacted by increasing drought and disturbance (Lindner et al., 2010). Net primary productivity (NPP) in these regions was expected to increase little, and in some cases to decrease, under climate change, so that many ecosystems may change from sinks to sources of C by 2100, mainly from drying caused by declining precipitation *vs*. rising evapotranspiration (Morales et al., 2007).

Ecosystem models used to study climate change impacts on seasonally dry grasslands need first to be tested for their ability to simulate ecological controls on NEP by simulating those on its component fluxes gross primary productivity (GPP) and ecosystem respiration (R_e) under highly variable rainfall. Of particular importance in this regard are the climatic and phenological signals initiating and terminating GPP and hence plant C uptake at the start and end of rainy seasons, and the effects of soil wetting and drying on C uptake and emission during rainy and dry seasons. In this study, we used the ecosystem model *ecosys* (Grant and Flanagan, 2007; Grant et al., 2006, 2007a,b,c, 2008, 2009) to test algorithms for:

(1) the climatic and phenological signals that induce germination during soil wetting at the start of the rainy season, and senescence during soil drying at the end of the rainy season, thereby setting the duration of GPP which enables sustained productivity by annual plants in seasonally dry climates,
(2) a soil–root–canopy–atmosphere hydraulic scheme by which soil and atmospheric water status determine plant water status, and hence GPP during soil wetting and drying between germination and senescence (Grant and Flanagan, 2007), and
(3) the stimulation or suppression of heterotrophic respiration (R_h) during wetting or drying of surface residues and soil (Grant and Rochette, 1994), thereby simulating the precipitation-driven pulses that characterize C emissions in seasonally dry ecosystems (Huxman et al., 2004).

CO_2 and energy fluxes modelled with these algorithms in *ecosys* were tested against those from continuous EC measurements recorded over an annual grassland from 2001 to 2008 in a Mediterranean climate zone at Vaira Ranch in California. Varying intensity and duration of rainy seasons recorded during this period provided a strong test of model robustness. These algorithms were then used to project changes in CO_2 fluxes and hence NEP for this grassland under different climate change scenarios projected for the next 100 years in California.

2. Methods

2.1. Model development

2.1.1. General

The key algorithms governing the modelling of ecological controls on NEP in *ecosys* are described in the Supplement to this article, in which equations and variables referenced in the Results below are described and listed in Appendices A, B, C and D. All model parameters in *ecosys* are derived from independent experiments and so remain unchanged in this study from those used in earlier studies (e.g. Grant et al., 2007b,c, 2008, 2009) as given in the Supplement. However these algorithms have not yet been tested under the more variable hydrological conditions encountered in Mediterranean ecosystems.

Algorithms (1), (2) and (3) above are described in more detail below.

2.1.2. Algorithm (1): initiation and termination of gross primary productivity in seasonally dry climates

Leafout and leafoff in cold-deciduous plant functional types (PFT) in *ecosys* occur when requirements for time accumulated at plant temperatures above or below set thresholds have been met under lengthening or shortening photoperiods respectively (e.g. Grant et al., 2009). Here we adapt this approach to leafout, or germination in annual plants, and senescence in drought-adapted PFTs by setting requirements for time accumulated at plant water potential above or below set thresholds to be met during earlier and later plant growth stages respectively. For this study time requirements and thresholds were set at 480 h above −0.2 MPa for germination, and 240 h below −2.0 MPa for senescence. These requirements were set to avoid premature germination or senescence and hence wastage of resources during false starts or ends to the rainy season. In the model, plant water potential is represented by canopy water potential (ψ_c), calculated from coupled equations by which root water uptake is equilibrated with canopy transpiration [B14]. When the canopy is absent before leafout in perennials or seed germination in annuals, ψ_c is determined by soil water potential (ψ_s) at seeding depth and so responds to rainfall events that maintain high ψ_s for long enough to meet the accumulated time requirements specified for the PFT.

During the growing season, ψ_c is determined by ψ_s throughout the rooted soil profile, and by transpirational demand imposed by vapor pressure deficit *D*. Therefore sustained declines in ψ_c that meet the time requirements for senescence occur only when most of the rooted soil profile is dry and *D* is large. Sustained declines in ψ_c also induce senescence and litterfall through declining CO_2 fixation and consequent depletion of nonstructural C products by respiration and grain filling. This depletion forces remobilization of metabolic C and litterfall of associated structural C to meet respiration and grain filling requirements. Senescence in the model drives translocation of plant nonstructural C to storage reserves (perennials) or seeds (annuals) that drive regrowth following leafout or germination at the start of the next growing season. These processes for leafout and senescence were designed in the model to maximize long-term productivity of drought-adapted plants under variable rainfall. This was accomplished by using nonstructural C during favourable growing conditions to grow and maintain structural C required to produce storage or seed C, while limiting wastage of nonstructural C during unfavourable growing conditions to grow and maintain structural C that does not produce storage or seed C.

Senescence modelled in annual plants may also be induced by phenological maturity following completion of their annual life cycle if this occurs before the senescence requirement for time accumulated at ψ_c below the set threshold has been met. The life cycle includes temperature-driven production of a set number of vegetative nodes followed by reproductive nodes that govern the timing of growth by vegetative and reproductive organs (Grant, 1989). Maturity in annual plants is achieved after seed growth ceases because seed sink capacity established during seed set has been filled, or because slow CO_2 fixation during unfavourable growing conditions has allowed nonstructural C pools used for respiration and grain filling to be depleted.

2.1.3. Algorithm (2): controls on gross primary productivity by soil and atmospheric water status

Canopy water status in *ecosys* is calculated hourly from a two-stage convergence solution for the transfer of water and heat through a multi-layered multi-population soil–root–canopy system. The first stage of this solution requires convergence to a canopy temperature T_c for each plant population at which the closure of the canopy energy balance (net radiation R_n, sensible heat flux H, latent heat flux LE and change in heat storage G) is achieved. After convergence for T_c, a value is sought for ψ_c at which canopy transpiration from the closed energy balance equals total water uptake from all rooted soil layers (Grant, 1998) plus changes in plant water content. Because the new value of ψ_c may alter stomatal resistance r_c and hence LE in the energy balance, sequential convergences for T_c and ψ_c are repeated until successive changes fall below an acceptance threshold. This solution is more fully described and tested in Grant and Flanagan (2007).

After convergence for T_c and ψ_c, CO_2 fixation V_c is calculated under ambient ψ_c and r_c from non-stomatal and stomatal constraints on CO_2- and light-limited carboxylation (Grant and Flanagan, 2007). The calculation of V_c is accomplished through a convergence solution for C_i and its aqueous counterpart C_c at which diffusive and biochemical fluxes equilibrate (Grant and Flanagan, 2007). The CO_2 fixation rate of each leaf surface at convergence is added to arrive at a value for canopy GPP and hence C uptake by each plant population in the model. During soil drying, declining ψ_s and increasing soil and root resistances force lower ψ_c to maintain water potential gradients required for soil–root–canopy uptake to meet transpiration driven by LE. Lower ψ_c eventually forces higher r_c and hence lower LE, while lower ψ_c and higher r_c impose increasing constraints on V_c.

2.1.4. Algorithm (3): controls on heterotrophic respiration by soil water status

Organic transformations in *ecosys* occur in five organic matter–microbe complexes (coarse woody litter, fine non-woody litter, animal manure, particulate organic carbon (POC), and humus), each of which consists of five organic states (solid organic matter, dissolved organic matter, sorbed organic matter, microbial biomass, and microbial residues) in a surface residue layer and in each soil layer. The decomposition rate of each state in each complex is a first-order function of the active biomass M of heterotrophic microbial populations, including obligate aerobes, facultative anaerobes, fungi, fermenters, acetotrophic methanogens, as well aerobic and anaerobic diazotrophs, and a Monod function of substrate concentration, calculated from the fraction of substrate mass colonized by M. The product of decomposition is dissolved organic C (DOC) which is the substrate for R_h that drives microbial growth. The decomposition rate is also controlled by T_s through an Arrhenius function and by soil water content (θ) through its effect on aqueous microbial concentrations [M]. Values of T_s and θ are calculated from surface energy balances and from heat and water transfer schemes through atmosphere–canopy–snow–surface residue–soil profiles. When θ declines with drying of surface residue or soil, [M] rises, slowing decomposition and hence the production of DOC, slowing R_h and hence growth of M, and thereby further slowing decomposition. Conversely when θ rises with wetting of surface residue or soil, [M] declines, hastening decomposition and production of DOC, thereby hastening R_h, growth of M, and further hastening decomposition.

Table 1

Representative properties of the Exchequer very rocky silt loam at the Vaira Ranch site used in *ecosys*.

Horizon	A	B	C1	C2
Depth to bottom (m)	0.10	0.35	0.50	0.75
Bulk density (Mg m^{-3})	1.43	1.43	1.43	1.43
Field capacity (m^3 m^{-3})[a]	0.256	0.306	0.306	0.277
Wilting point (m^3 m^{-3})[a]	0.086	0.116	0.116	0.104
Ksat (mm h^{-1})[a]	43.2	28.8	28.8	12.8
Sand (g kg^{-1})	290	290	290	290
Silt (g kg^{-1})	580	580	580	580
Clay (g kg^{-1})	130	130	130	130
Coarse fragments (m^3 m^{-3})	0	0	0.50	0.75
Organic C (g kg^{-1})	13.9	13.9	1.4	1.4
Total N (g Mg^{-1})	1400	1400	140	140

[a] Derived from Saxton et al. (1986) and Baldocchi et al. (2004).

This DOC is the substrate for R_h by all M in each substrate-microbe complex in the surface residue and each soil layer. Rates of R_h may be constrained by microbial N or P concentrations, DOC, T_s, O_2 and ψ_s. The constraint by ψ_s is important only for zones in close contact with the atmosphere, such as the surface residue and surface soil layers, in which very low ψ_s can occur with prolonged drying. Total R_h from all organic states in all complexes in the surface residue and in the soil layers drives CO_2 emission from the soil and residue surfaces through volatilization and diffusion.

Organic transformations in *ecosys* are more fully described and tested in Grant et al. (1993a,b), Grant and Rochette (1994), Grant et al. (2007c) and in other papers cited below. At this stage of model development, photodegradation of surface residues (Rutledge et al., 2010) is not modelled because of uncertainty in parameterization.

2.2. Model experiment

2.2.1. Site description

CO_2 and energy fluxes were measured by EC from 2001 to 2008 over an open, lightly grazed grassland, dominated by cool-season C_3 annual species (grasses, forbs and legumes), on an Exchequer very rocky silt loam (Lithic xerorthents; Table 1), under a Mediterranean climate (mean annual temperature 16.3 °C, precipitation 559 mm) at the Vaira Ranch (38.418N, 120.958W) in California, USA. Interannual variation in precipitation measured during this period was found to be representative of that in long-term historical weather data from the region in which Vaira Ranch is located. Site characteristics and EC methodology are described in greater detail by Baldocchi et al. (2004), Ma et al. (2007), and Xu and Baldocchi (2004).

2.2.2. Model initialization and spinup

Site conditions were simulated by initializing *ecosys* with the biological properties of annual grasses and legumes, the key plant functional types (PFTs) at Vaira Ranch. These PFTs differed only in phenological attributes associated with monocot *vs.* dicot and determinate *vs.* indeterminate growth habits, and in symbiotic nitrogen fixation by legumes as described for soybean in Grant et al. (2007a). Otherwise the biological properties of these PFTs were identical, and remained unchanged from those used in earlier modelling studies (e.g. Grant, 1989; Grant and Flanagan, 2007; Grant et al., 2007a) as given in the Supplement. These PFTs competed for common resources of radiation, water and nutrients during each growing season, based on their vertical distributions of leaf area and root length driven by C fixation and allocation. *Ecosys* was also initialized with the physical and chemical properties of the soil (Table 1), and the topographic properties of the landscape of the open grassland at Vaira Ranch. The model was then run from a modelled date of 1 January 1874 to a modelled date of 31 December 2008 under repeating sequences of continuous hourly weather data (radiation, T_a, RH, wind speed and precipitation) recorded at Vaira Ranch from 1 January 2000 to 31 December 2008 (i.e. 15 cycles of 9 years). This run was long enough for C and energy cycles in the model to attain equilibrium under the Vaira Ranch site conditions well before the period of model testing from 2001 to 2008.

The two annual PFTs were seeded during the first year of the model run (nominally 1874). During subsequent growth they set and filled seeds at rates determined by their C, nutrient and water status during pre- and post-anthesis growth periods (e.g. Grant, 1989; Grant et al., 2007a, 2011). The PFTs then senesced at the end the growing season as described under Model Development above, at which time their seed numbers and masses contributed to those of soil seed banks. The seed numbers and masses in the soil seed banks then drove germination at the start of the next growing season. The timing of anthesis in the PFTs (Grant, 1989) was set so that sufficient grain C allocation had occurred by the end of most growing seasons to maintain seed banks large enough to drive germination and early growth at the start of the following rainy season. Apart from CO_2 fixation, no further C was added to drive plant growth after the initial seeding, so that both PFTs depended entirely upon self-seeding after the first year. During the model run, atmospheric CO_2 concentration (C_a) rose exponentially from 275 μmol mol^{-1} to 385 μmol mol^{-1}, NH_4^+ and NO_3^- concentrations in precipitation used to simulate wet N deposition were maintained at 0.50 and 0.25 g N m^{-3} (National Atmospheric Deposition Program), and NH_3 concentration in the atmosphere used to simulate dry N deposition was maintained at 0.005 μmol mol^{-1}. The timing and intensity of grazing at the field site was not recorded, but was considered to be infrequent and low, so that grazing was not applied in the model.

2.2.3. Model testing

NEP from *ecosys* simulated after 130 model years was compared at hourly, daily and seasonal time scales with that measured from 2001 to 2008 by the EC flux tower over the open grassland at Vaira Ranch, and gap-filled according to protocol described in Ma et al. (2007). Model performance in each year was evaluated from regressions of modelled hourly CO_2 and LE fluxes on measured hourly averaged EC CO_2 and LE fluxes in which both (1/2)-hourly values were considered accurate. Evaluations were based on intercepts ($a \to 0$), slopes ($b \to 1$), correlation coefficients ($R^2 \to 1$), and on comparisons of root mean squares for differences between EC and modelled fluxes (RMSD) *vs.* root mean squares for error in EC fluxes (RMSE). Values of RMSE for each year were calculated as the pooled root mean square of uncertainty in (1/2)-hourly EC fluxes during the year using equations for random measurement errors of CO_2 and LE fluxes derived over a grassland by Richardson et al. (2006).

2.2.4. Model projections

The model run used for testing from 2001 to 2008 was then extended for a further 135 years under constant 2008 C_a and repeating sequences of the 2000–2008 weather data recorded at Vaira Ranch to identify any long-term changes in model output not attributed to climate change. Results from this run were compared to those from extended runs in which C_a and the 2000–2008 weather sequence were altered hourly by climate change factors taken from Meehl et al. (2007) and Hayhoe et al. (2004) for the SRES A1fi and B1 emission scenarios under the medium-sensitivity UKMO Hadley Centre Climate Model V.3 (HadCM3) for seasonal temperature and precipitation in California (Table 2). During these runs NH_4^+ and NO_3^- concentrations in precipitation and NH_3 concentration in the atmosphere remained at values used in the model run under current climate. Model results for NEP from these extended runs under A1fi and B1 were compared with those under current climate.

3. Results

3.1. Modelled vs. measured CO_2 and energy fluxes

Regressions of modelled on measured hourly CO_2 fluxes during each year from 2001 to 2008 indicated that the model reproduced variation in the measured values (slope *b* close to one) with only small biases (intercept *a* less than RMSE, and also similar to or less than the zero flux detection limit of *ca.* 0.3 μmol m^{-2} s^{-1} for EC measurements at the study site) for each of the years in the study (Table 3a). Modelled and measured CO_2 fluxes were sufficiently well correlated (R^2 from 0.72 to 0.88, except for 2008) that the RMSD of ~2 μmol m^{-2} s^{-1} could be attributed to a general estimate of 20% for random error in EC flux measurements (Wesely and Hart, 1985). However this RMSD was about twice as large as RMSE estimated from measured fluxes, suggesting the possibility of closer agreement between EC and modelled CO_2 fluxes, even though model bias was small.

Regressions of modelled on measured LE fluxes indicated that the model reproduced variation in EC measurements from 2001 to 2008 (*b* close to 1.0) with little bias (*a* less than RMSE) (Table 3b). Correlations were high enough in all years (R^2 from 0.67 to 0.90) that RMSD from the regressions was smaller than RMSE. Regression results in Table 3b indicated that closer agreement between EC and modelled LE fluxes was unlikely to be achieved without further reducing uncertainty in the EC measurements.

3.2. Seasonal controls on CO_2 exchange under current climate

CO_2 exchange was strongly limited by soil drying during the hot dry summers at Vaira Ranch (Fig. 1) which terminated NPP and greatly reduced R_h. In the model, this limitation on R_h was imposed when low θ raised aqueous concentrations of microbial biomass ($[M] = M/\theta$ in [A3, A4]), thereby reducing specific decomposition activity [A1, A2]. This reduced activity slowed DOC production which further reduced R_h [A13] which drove microbial growth [A19–A25]. A further limitation on R_h was imposed by the effects of low ψ_s during extreme soil drying [A13, A15].

These limitations on R_h were suddenly alleviated by the onset of the rainy season in October or early November, causing rapid rises in θ and hence in CO_2 emissions (Fig. 1). In the model, these rises were driven by rapid declines in $[M]$ and rises in ψ_s with wetting of the surface residue and soil, which accelerated decomposition and DOC production [A1, A2], R_h [A3, A4, A13, A15] and hence microbial growth [A19–A25], which further accelerated decomposition. The large diurnal variation in CO_2 emissions modelled with wetting was driven by large diurnal variation in surface residue temperature caused by radiative heating and cooling of surface residue with only limited buffering from heat exchange with the soil surface underneath. On some days, diurnal variation in CO_2 effluxes from the model was larger than that measured by EC, although daily total effluxes were similar (Fig. 1). These interactions among key processes driving R_h allowed modelled CO_2 effluxes to rise rapidly after precipitation events at the onset of the rainy season (Fig. 2a, b), and to decline rapidly with drying thereafter (Fig. 2c, d). At the current stage of model development, the pulse of CO_2 emitted after rainfall events was not primed by prior photodegradation of surface residue (e.g. Rutledge et al., 2010).

These CO_2 effluxes were gradually offset by rising influxes from CO_2 fixation by annual vegetation regrowing from seed, so that the ecosystem remained a C source (NEP < 0) until mid to late January.

Table 2
Annual changes in seasonal air temperatures (T_a) and precipitation predicted from 1961–1990 to 2090–2099 by the UKMO Hadley Centre Climate Model V.3 (HadCM3), and in atmospheric CO$_2$ concentrations (C_a) for the SRES A1fi and B1 emission scenarios in California (from Hayhoe et al., 2004 and Meehl et al., 2007).

	T_a, °C y^{-1}	Precip., y^{-1}	C_a, y^{-1}	T_a, °C y^{-1}	Precip., y^{-1}	C_a, y^{-1}
Scenario		A1fi			B1	
December–February	0.0364	0.9962	1.00866	0.0209	0.9968	1.00324
March–May	0.0496	0.9974	1.00866	0.0286	0.9987	1.00324
June–August	0.0755	0.9995	1.00866	0.0418	0.9974	1.00324
September–November	0.0496	0.9974	1.00866	0.0286	0.9987	1.00324

In the model, these slow rises in CO$_2$ fixation following the start of the rainy season were caused by (1) delayed seed germination until the time requirement at ψ_c (=ψ_s) above the set threshold for germination was met, and (2) slow initial plant growth driven from seed bank reserves during germination in cool soils, causing slow early growth in leaf area [C21] and root length [B13] and hence slow gains in light [C7] and nutrient [A37] acquisition, thereby slowing further growth in leaf area and root length, and hence in CO$_2$ fixation and nutrient uptake. Rises in CO$_2$ fixation during 2008 were delayed after an unusually early start to the rainy season in autumn 2007 was followed by a protracted dry period (Fig. 1s). This early dry period may have reduced germination more than was modelled (Fig. 1x), and hence may have caused the overestimation of measured CO$_2$ fluxes by the model in Table 3a.

As the rainy season progressed, NPP from rising CO$_2$ fixation eventually exceeded R_h, causing the ecosystem to become a net C sink (NEP > 0) with greater T_a, precipitation, θ and daylength after late January (Fig. 1). However NPP declined rapidly with θ following the onset of the dry season in April or May. In the model, soil drying reduced ψ_s, raised soil and root hydraulic resistances (Ω_s and Ω_r) [B9] and hence slowed root water uptake [B6], forcing lower ψ_c [B14] and ψ_t [B4], and eventually higher r_c [B3] to meet increasing transpiration requirements imposed by the effects of rising T_a and D on LE [B1]. Higher r_c and lower ψ_c reduced CO$_2$ fixation and hence NPP through combined stomatal [C2] and non-stomatal [C9] processes. Reduced CO$_2$ fixation caused depletion of nonstructural C products needed to meet requirements for maintenance respiration and grain filling, forcing more rapid remobilization of metabolic C in leaves and roots, and hence litterfall of associated structural C [C18], which reduced LAI and hence further reduced CO$_2$ fixation. Remobilization was further hastened once time accumulated at ψ_c below the set threshold had been exceeded in years with an earlier end to the rainy season (e.g. 2004 in Fig. 1j), or when seed growth had been completed in years with a later end to the rainy season (e.g. 2005 in Fig. 1m). In these later years, NEP declined earlier than did θ (Fig. 1o *vs.* n), indicating phenology-driven senescence.

Annual NEP was therefore determined by the comparative durations and intensities of net C emission when R_h exceeded NPP, mostly during November to January, *vs.* net C uptake when NPP exceeded R_h, usually during January to May (Fig. 1). The duration of net C uptake varied with the time at which the rainy season began and ended each year. Ma et al. (2007) reported that green-up following the onset of the rainy season was late in autumn 2003 and early in autumn 2004, while senescence following the end of the rainy season was early in spring 2004 and late in spring 2005. Consequently the length of the growing season was shortest in 2003–2004 and longest in 2004–2005 during the study period, so that CO$_2$ and energy exchange measured during these years provided a test of model robustness under contrasting seasonal weather. Later soil wetting in autumn 2003 *vs.* 2004 (Fig. 1h *vs.* k) delayed germination and early leaf area growth in the model [C21], causing less rapid CO$_2$ uptake to be measured and modelled [C1] under comparable weather (Fig. 3a *vs.* d) during warming in early March of 2004 *vs.* 2005 (Fig. 3c *vs.* f), and hence a slower rise in winter NEP (Fig. 1l *vs.* o). Earlier soil drying in spring 2004 *vs.* 2005 hastened the onset of water stress, lowering ψ_c [B14] and so reducing LE and CO$_2$ fluxes measured and modelled [B1, C1] during late spring 2004 *vs.* 2005 (Fig. 3h, i *vs.* k, l), causing an earlier decline

Table 3
Intercepts (a), slopes (b), coefficients of determination (R^2), root mean square of differences between modelled and measured fluxes (RMSD), root mean square of error in measured fluxes (RMSE) calculated for a grassland site by Richardson et al. (2006), and number of accepted eddy covariance (EC) fluxes (n) from regressions of hourly modelled (a) CO$_2$ and (b) LE fluxes *vs.* hourly-averaged fluxes measured from 2001 to 2008 at Vaira Ranch, CA. All measured fluxes are hourly averages of two accepted (1/2)-hourly values.

Year	a[a]	b	R^2	RMSD	RMSE	n
(a)				**CO$_2$ fluxes**		
	μmol m^{-2} s^{-1}			μmol m^{-2} s^{-1}	μmol m^{-2} s^{-1}	
2001	0.0	0.95	0.75	2.4	1.2	4610
2002	0.0	0.98	0.84	1.9	1.1	4780
2004	0.2	1.11	0.77	1.9	1.0	3742
2005	0.2	1.06	0.88	2.4	1.4	4095
2006	−0.1	0.93	0.72	2.2	1.0	4430
2007	0.4	1.10	0.81	2.1	1.1	4152
2008	0.0	1.21	0.51	1.5	0.8	5932

Year	a[a]	b	R^2	RMSD	RMSE	n
(b)				**LE fluxes**		
	W m^{-2}			W m^{-2}	W m^{-2}	
2001	2.2	1.00	0.73	28	25	5933
2002	2.5	1.08	0.84	19	28	6893
2003	−0.2	1.06	0.80	22	29	6554
2004	−1.5	1.01	0.70	26	31	5271
2005	3.2	1.17	0.90	20	33	5856
2006	−0.3	0.98	0.81	23	30	5931
2007	0.3	1.16	0.86	20	29	5135
2008	−0.3	1.00	0.67	23	27	6041

[a] a, b and R^2 from regressions of modelled on measured fluxes, RSMD from regressions of measured on modelled fluxes.

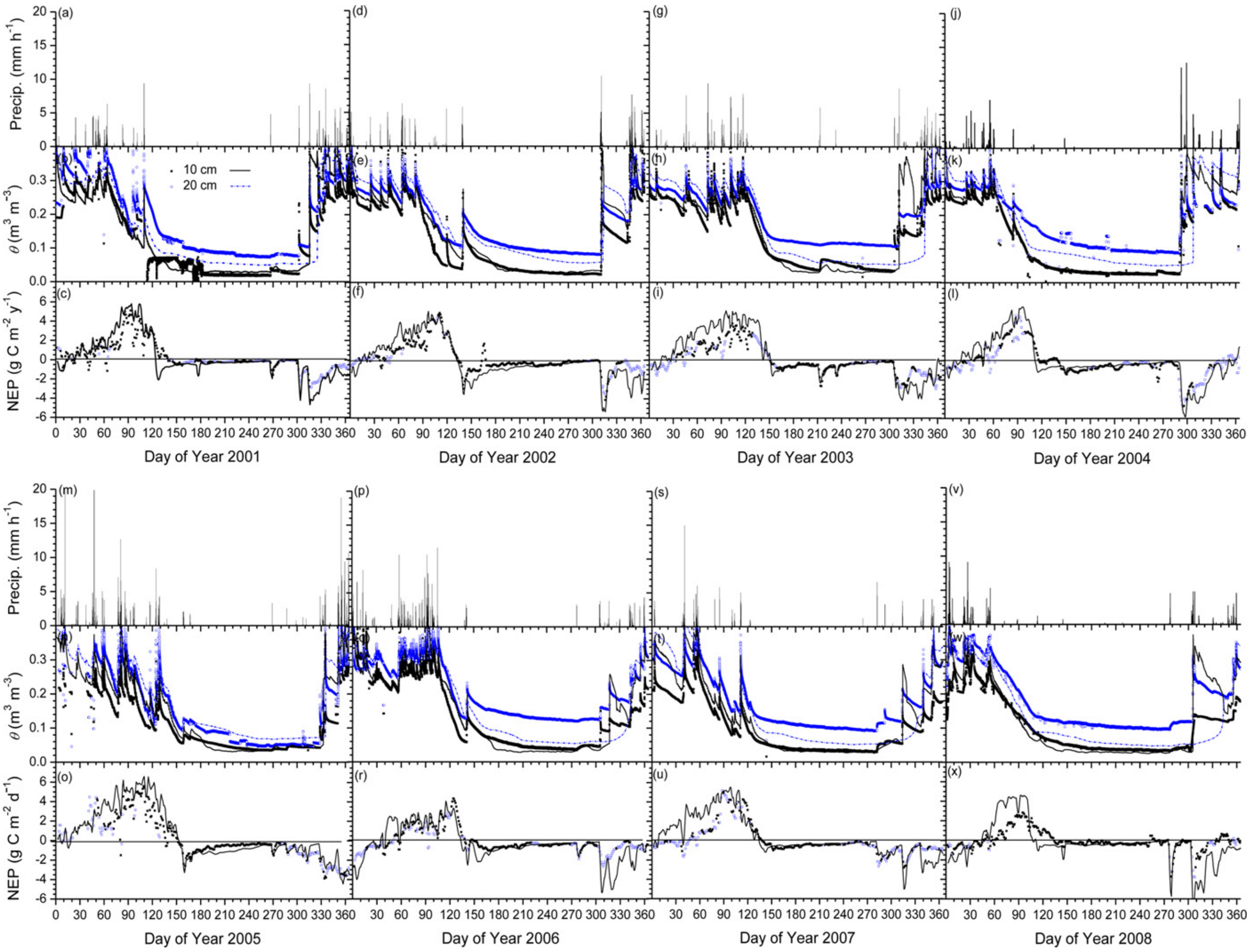

Fig. 1. Precipitation, soil water content at 0.10 and 0.20 m (θ) and net ecosystem productivity (NEP) 3-day moving averages measured (symbols) or modelled (lines) from 2001 to 2008 at Vaira Ranch, CA. Positive or negative values for NEP denote net C uptake or emission respectively. Open symbols for NEP represent daily values consisting of >24(1/2)-hourly gap-filled fluxes.

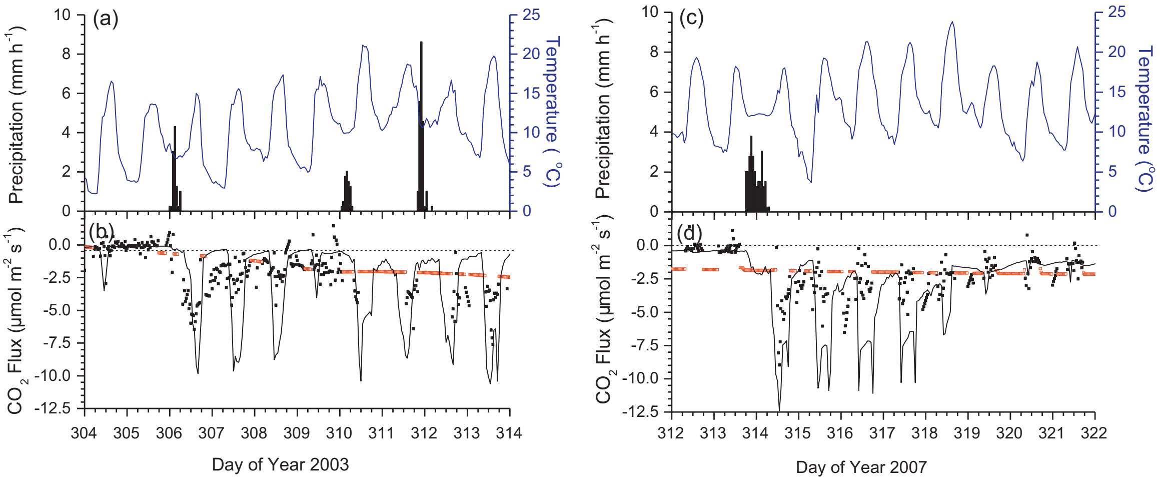

Fig. 2. (a, c) Precipitation and air temperature recorded, and (b, d) CO_2 fluxes measured (symbols) and modelled (lines) at Vaira Ranch, CA before, during and after the start of the rainy season on (a, b) DOY 307 in 2003 and (c, d) DOY 315 in 2007. Positive values denote downward fluxes, negative values upward. Open symbols for CO_2 fluxes represent gap-filled values.

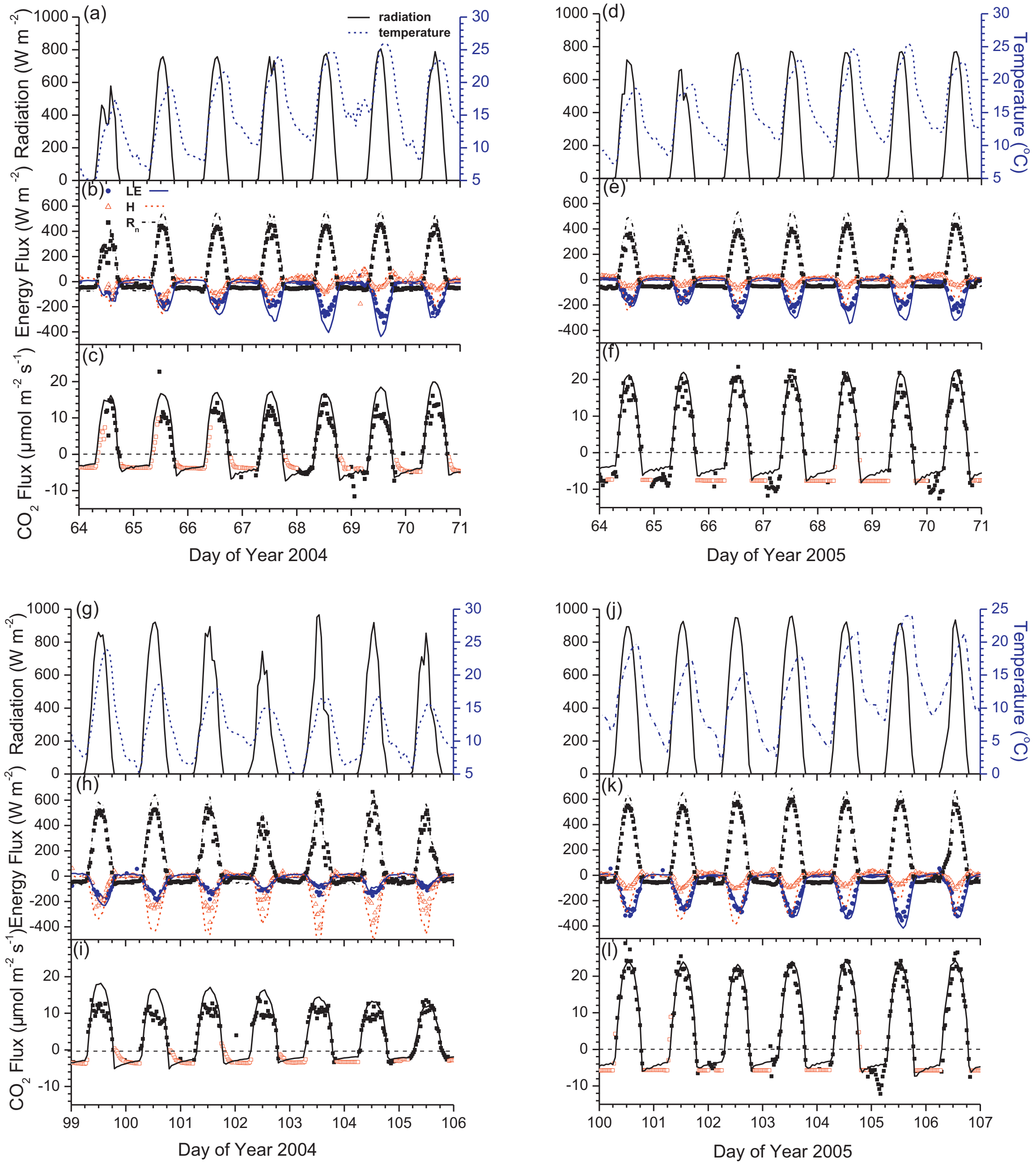

Fig. 3. Solar radiation and air temperature recorded, and energy and CO_2 fluxes measured (symbols) and modelled (lines) at Vaira Ranch, CA from DOY 65 to 71 and from DOY 101 to 107 in 2004 and 2005. Positive values denote energy or CO_2 influxes, negative values energy or CO_2 effluxes. Open symbols for CO_2 fluxes represent gap-filled values.

in spring NEP (Fig. 1l *vs.* o). The earlier rise and later decline in CO_2 uptake during 2005 *vs.* 2004 were clearly apparent in the average diurnal CO_2 fluxes measured and modelled during 3-week periods in early March and late April (Fig. 4) that included the 1-week periods shown in Fig. 3.

3.3. Seasonal controls on annual net ecosystem productivity

The hydrological year for Mediterranean climate zones in California can be considered to start and finish at the end of successive dry seasons (e.g. DOY 295 in Ma et al., 2007) so that productivity during the entire growing season can be included in a single year. The later rise and earlier decline of net C uptake with the shorter growing season in 2004 (Figs. 1l and 3c, i) caused modelled and EC-derived annual GPP to be smaller than in the other years of this study except for 2008, while the earlier rise and later decline of net C uptake with the longer growing season in 2005 (Figs. 1o and 3f, l) caused modelled and EC-derived annual GPP to be larger (Table 4). In the model, R_a varied with GPP so that interannual variation in NPP followed that in GPP.

Later wetting and earlier drying in 2003–2004 also lowered annual R_h, while earlier wetting and later drying in 2004–2005 raised annual R_h (Table 4; Fig. 1). Litterfall from the larger NPP in 2004–2005 increased litter C stocks, the subsequent decomposition of which caused the comparatively high R_h, R_e and hence low NEP modelled and derived from EC measurements during 2005–2006 (Table 4). Less litterfall from the smaller NPP in 2005–2006 caused the comparatively lower R_h, R_e and hence higher NEP modelled and

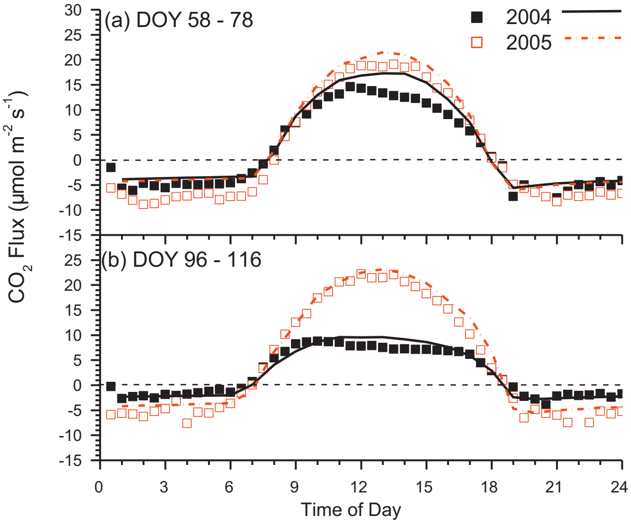

Fig. 4. Average diurnal CO_2 fluxes measured (symbols) and modelled (lines) at Vaira Ranch, CA from DOY 58 to 78 and from DOY 96 to 116 in 2004 and 2005. Positive values denote CO_2 influxes, negative values CO_2 effluxes.

derived from EC measurements during 2006–2007 (Table 4). These lags in litterfall decomposition *vs.* production contributed to rises and declines in NEP during alternate years. Interannual variability in modelled R_h was smaller than that in NPP, so that R_h was greater than NPP in years with shorter rainy seasons (NEP < 0), but less than NPP in years with longer rainy seasons (NEP > 0) (Table 4).

Annual NEP in the model was consistently larger than that derived from EC measurements (Table 4), even though modelled and measured CO_2 fluxes corresponded well (Table 3a). This larger NEP arose from smaller modelled *vs.* EC-derived R_e relative to GPP (Table 4), caused by smaller modelled *vs.* gap-filled CO_2 effluxes during nights when inadequate atmospheric turbulence required replacement of measured values (e.g. Fig. 3f, l). These smaller values occurred when modelled effluxes declined with soil cooling during nights while gap-filled values remained constant. The larger modelled *vs.* EC-derived NEP could also be partly attributed to dry-season photodegradation of surface residues, estimated by Rutledge et al. (2010) to be 16 g C m^{-2} at the Vaira Ranch grassland site during the 2007 dry season, but not accounted for in the model. EC-derived NEP could have been further reduced by grazing at the field site which was not applied in the model, although grazing was thought to be light.

Losses of dissolved inorganic and organic C in runoff and drainage water caused total NEP in the model to be less than NEP calculated from CO_2 exchange (Table 4). This water would likely have degassed elsewhere, but might have contributed to CO_2 fluxes within the tower fetch if such water was also entering the fetch from higher topographic positions. Average NEP ± interannual variation from 2001 to 2008 was +29 ± 110 g C m^{-2} y^{-1} (modelled) *vs.* −34 ± 102 g C m^{-2} y^{-1} (EC-derived). Interannual variation in modelled and EC-derived NEP was well correlated ($R^2 = 0.75$, $P < 0.005$) and consistent in direction (sink *vs.* source) (Table 4). This NEP was modelled without grazing, fire, insects or other disturbances that may occur in these grassland ecosystems, and so was larger than the net biome productivity (NBP) that would have been modelled had these disturbances been represented (e.g. Grant et al., 2006). Annual peak above-ground phytomass in the model varied from 220 g C m^{-2} in 2008 to 380 g C m^{-2} in 2005, of which 25–30% was legume. The legume composition in the model was slightly larger than the upper range of 20% found by Pitt and Heady (1978) in California annual grasslands.

3.4. *Seasonal net ecosystem productivity projected under climate change*

Changes in temperature and precipitation under SRES A1fi and B1 (Table 2) caused gradual changes in modelled ecosystem productivity. These changes are examined at a diurnal time scale in Fig. 5 under weather derived after 99 years of climate change (11 cycles of incremented 2000–2008 weather), and at a seasonal time scale in Fig. 6 under weather derived after 54 and 99 years of climate change (6 and 11 cycles of incremented 2000–2008 weather). Diurnal *LE* changed little from current rates (the same as those modelled in 2004 and 2005 in Fig. 3b, e) under B1 and declined under A1fi (Fig. 5b, e) because reductions in transpiration from greater r_c under rising C_a (Fig. 5a) [B2] offset increases in evapotranspiration from greater *D* under rising T_a (Fig. 5a) [B1] (Grant et al., 1999), thereby avoiding more rapid water use under climate change. Also increases in surface evaporation under higher T_a sometimes hastened drying of surface residue which reduced subsequent surface evaporation (e.g. DOY 69 and 70 in Fig. 5b). Diurnal CO_2 influxes rose above current rates (the same as those modelled in 2004 and 2005 in Fig. 3c, f) under B1 and further under A1fi because increases in CO_2 fixation under rising C_a [C6], T_a [C6, C7, C10] and LAI [C21] were only partly offset by much smaller increases in CO_2 effluxes from more rapid R_h [A11] with rising soil temperature (T_s) [A1, A2, A5, A13] (Fig. 5c, f). Diurnal CO_2 effluxes declined under climate

Table 4
Annual precipitation, length of growing season (LGS) and carbon balances modelled (M) or derived from eddy covariance (EC) (Ma et al., 2007) during hydrological years[b] ending in 2001 to 2008 at Vaira Ranch, CA.

Year	2001		2002		2003		2004		2005		2006		2007		2008	
Precip. (mm)	431		510		515		363		674		886		390		372	
	M	EC	M	EC	M	EC	M	EC	M	EC	M	EC	M	EC	M	EC
LGS (days)[a]	107	113	108	111	136	116	90	78	134	152	93	87	125	91	67	66
C budget									g C m^{-2} y^{-1}							
GPP	717	967	748	844	1058	993	673	626	1314	1313	782	813	913	756	473	362
R_a	238		261		367		226		453		289		324		152	
NPP	479		487		691		447		861		493		589		321	
R_h	415		507		529		470		685		593		470		397	
R_e	653	884	768	904	896	987	696	780	1138	1225	882	1002	794	655	549	484
NEP (CO_2)	+64	+83	−20	−61	+162	+6	−23	−154	+176	+88	−100	−189	+119	+101	−76	−122
NEP ±		50		53		51		49		61		51		63		31
DIC, DOC[c]	8		8		5		6		11		22		3		5	
NEP (total)	+56		−28		+157		−29		+165		−122		+116		−81	

[a] Number of days from the initiation to the termination of continuous daily net C uptake.
[b] From DOY 295 for comparison with GPP, R_e and NEP in Ma et al. (2007).
[c] Dissolved inorganic and organic C exported in runoff and drainage water.

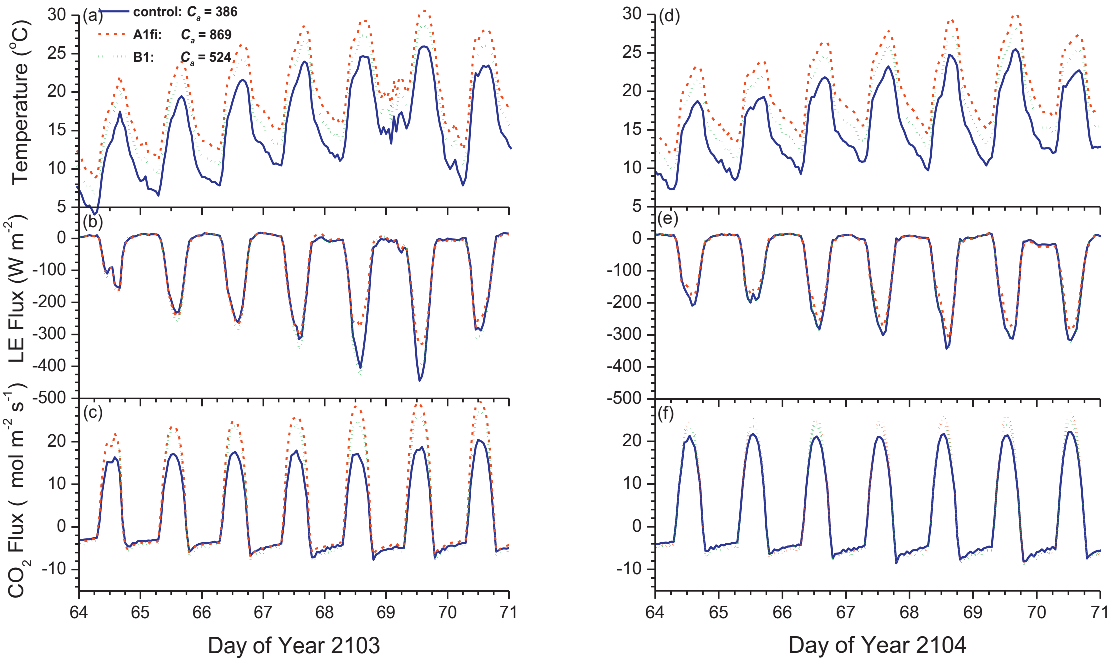

Fig. 5. (a, d) Air temperatures, (b, e) LE and (c, f) CO_2 fluxes modelled at Vaira Ranch, CA from DOY 65 to 71 in (a–c) 2103 and (d–f) 2104 with no climate change (control), and under climate change simulated by the UKMO Hadley Centre Climate Model V.3 (HadCM3) for the SRES A1fi and B1 emission scenarios in California (Table 2). Positive values denote energy or CO_2 influxes, negative values energy or CO_2 effluxes. Values of C_a indicate atmospheric CO_2 concentrations in μmol mol^{-1}.

change when surface residue dried more rapidly under higher T_a (e.g. DOY 69 and 70 in Fig. 5b).

At the seasonal time scale, rates of net C uptake during rainy seasons, and of net C emission during dry seasons, both rose as climate change progressed (Fig. 6a, b). Rises in net C uptake were caused by more rapid CO_2 fixation (Fig. 5c, f), and rises in net C emission were caused by more rapid R_h (Fig. 5c, f) from increased litterfall [C18] produced by greater net C uptake and hence NPP during previous and current rainy seasons. Seasonal rates of net C uptake and emission both rose more rapidly with greater warming under A1fi than B1 (Fig. 6). However the duration of seasonal net C uptake was shortened by two (B1) to four (A1fi) weeks in years with longer rainy seasons (e.g. years derived from 2003 or 2005 weather in Fig. 6) because warming hastened maturity and hence phenology-driven senescence of the annual PFTs. Consequently transpiration was terminated before the end of these longer rainy seasons (Fig. 1g, m), leaving longer periods of wet soil between senescence and summer drying. During these periods, C emissions rose, substantially reducing NEP. These more rapid emissions were caused by more rapid decomposition [A3, A4] and R_h [A11–A13], which drove more rapid N mineralization [A26], with soil wetting and warming. Consequent increases in mineral N availability raised NPP and hence NEP during the following rainy seasons (e.g. in years derived from 2004 or 2006 weather) (Fig. 5c).

The duration of net C uptake in the model was not much affected by climate change in years with shorter rainy seasons (e.g. years derived from 2004 weather in Fig. 6) because early soil drying (Fig. 1j) forced drought-driven senescence before maturity of the annual PFTs was reached, even with climate warming. Consequently the soil remained dry after senescence, reducing net C emission and N mineralization. These reductions avoided large losses in NEP during the current year, but limited rises in NPP and hence NEP during the following year (e.g. in years derived from 2005 weather) (Fig. 5f). Therefore annual NEP of years with longer rainy seasons tended to decline during climate change, while that of years with shorter rainy seasons tended to rise. These changes in annual NEP progressed more rapidly with greater warming under A1fi *vs.* B1 (Fig. 6).

3.5. *Centennial net ecosystem productivity under climate change*

Under current climate, interannual variation in precipitation (Fig. 7a) was greater than that in evapotranspiration (ET) (Fig. 7b), and so drove interannual variation in surface runoff plus subsurface drainage (Fig. 7c), with larger values modelled during rainier years such as 2005 and 2006 (Table 4). During climate change, interannual variation in precipitation was maintained (Fig. 7a) but values gradually declined, more so under A1fi than under B1 (Table 2). However ET changed little due to the offsetting effects of rising C_a [B2] and T_a [B1] on transpiration at diurnal (Fig. 5b, e) and hence annual (Fig. 7b) time scales. Consequently runoff plus drainage also

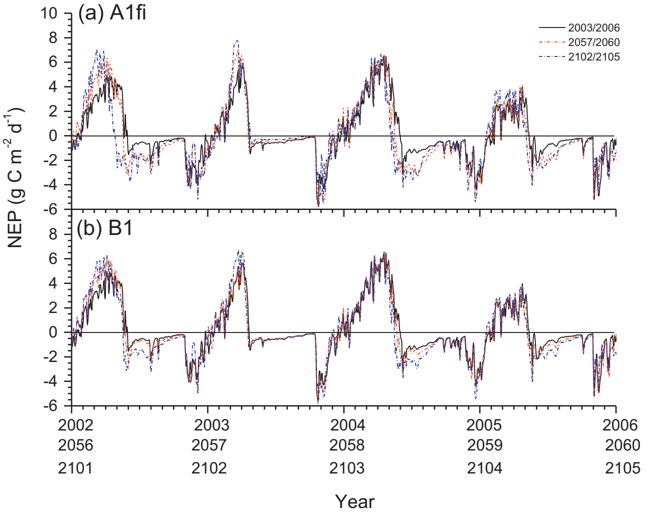

Fig. 6. Net ecosystem productivity (NEP) 3-day moving averages modelled from 2003 to 2006 (where 2003.0 indicates the end of 2003), and under 2003–2006 weather altered hourly over 54 years (2057–2060) and 99 years (2102–2105) under climate change simulated by the UKMO Hadley Centre Climate Model V.3 (HadCM3) for the SRES (a) A1fi and (b) B1 emission scenarios in California (Table 2). Positive values denote net CO_2 uptake, negative values net CO_2 emission.

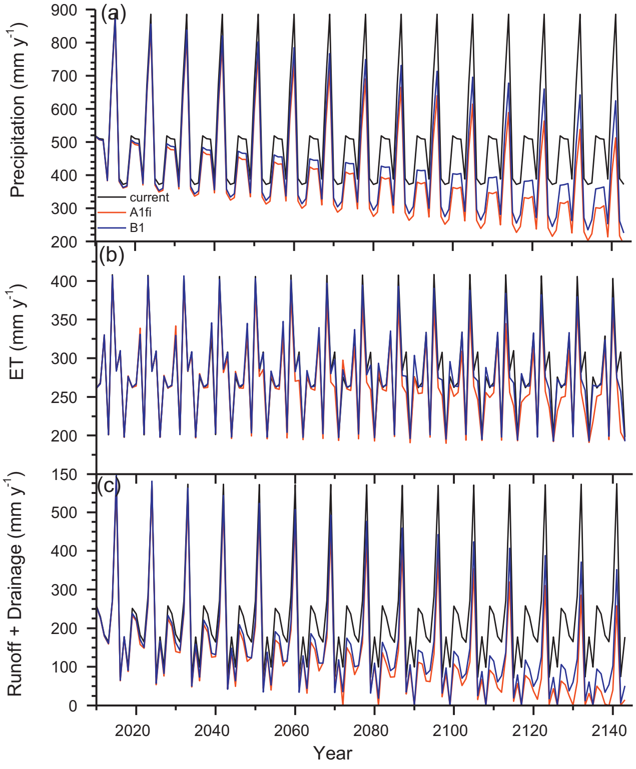

Fig. 7. (a) Precipitation, (b) evapotranspiration (ET) and (c) surface runoff plus subsurface drainage modelled during hydrological years (from DOY 295) under current climate (2000–2008), and under climate change scenarios from the UKMO Hadley Centre Climate Model V.3 (HadCM3) under SRES A1fi and B1 (Table 2) from 2010 to 2143.

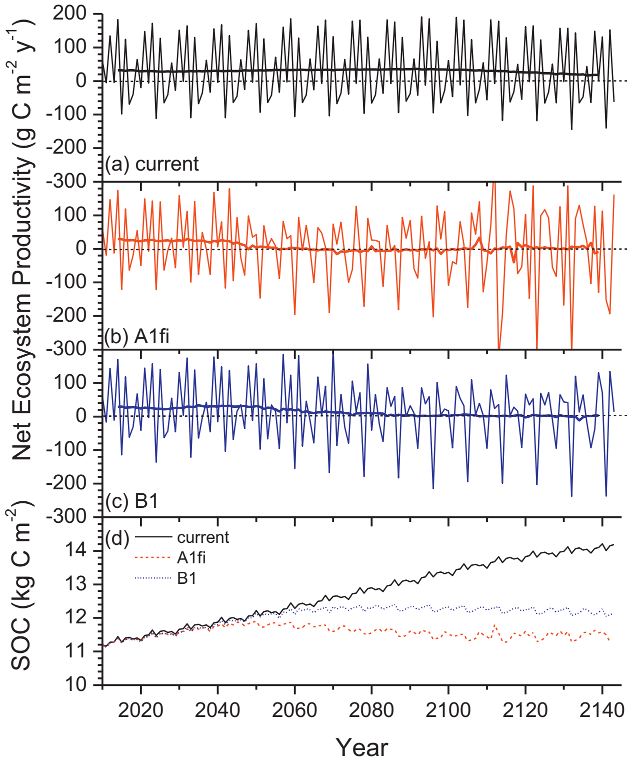

Fig. 8. (a–c) Annual and 9-year moving average net ecosystem productivity (NEP) and (d) soil + litter C modelled during hydrological years (from DOY 295) under current climate (2000–2008), and under climate change scenarios from the UKMO Hadley Centre Climate Model V.3 (HadCM3) under SRES A1fi and B1 (Table 2) from 2009 to 2143.

declined, more under A1fi than under B1, reaching zero during drier years after 100 years of climate change (Fig. 7c).

Interannual variation in NEP modelled under current climate (Table 4) was maintained during the extended model run from 2010 to 2142 (Fig. 8a), with positive values modelled under longer rainy seasons in 2003, 2005 and 2007, and negative values under shorter rainy seasons in 2002, 2004 and 2006. Average NEP remained at that modelled under current climate until a slight decline towards the end of the run was caused by a gradually developing phosphorus deficiency. Consequently SOC modelled under current climate rose steadily during the extended model run (Fig. 8d).

The pattern of interannual variation in NEP modelled under current climate was maintained during the first 30 years under A1fi (Fig. 8b) and 50 years under B1 (Fig. 8c), but changed thereafter as NEP rose in years with shorter rainy seasons, and declined in years with longer. This change was driven by rises in net C emissions that exceeded those in net C uptake (Fig. 6), so that average NEP declined towards zero as this change developed. However this decline was small with respect to interannual variation in NEP, so that most annual values modelled during climate change remained within the range of those under current climate. The pattern of interannual variation in NEP changed again after 100 years under A1fi (Fig. 8b) and 130 years under B1 (Fig. 8c), with larger C sinks or sources occurring in some years, although average NEP remained near zero. SOC modelled under A1fi and B1 stopped rising as NEP declined, and fell gradually thereafter (Fig. 8d) with continued DOC losses (Table 4). After 100 years of climate change, annual peak above-ground phytomass modelled under A1fi varied from 250 to 370 g C m^{-2}, of which only 2% was legume, and under B1 from 245 to 375 g C m^{-2}, of which 5% was legume. This peak phytomass was similar to that modelled under current climate, but consisted of more grass and less legume.

4. Discussion

4.1. Net ecosystem productivity under current climate

Variable rainy seasons cause large interannual variation in NEP of seasonally dry grasslands in Mediterranean climate zones. The range in annual NEP (CO$_2$) of +176 to −100 g C m^{-2} y^{-1} modelled at Vaira Ranch (Table 4) was similar to one of +190 to–49 g C m^{-2} y^{-1} derived from EC measurements by Pereira et al. (2007) over a grassland under a similar Mediterranean climate in Portugal. Annual NEP at Vaira Ranch was not correlated with total precipitation (modelled: $R^2 = 0.01$, $P = 0.8$; EC: $R^2 = 0.05$, $P = 0.6$ in Table 4), much of which fell during winter when ET was low (e.g. Fig. 3b, e) and θ was high (Fig. 1). Greater precipitation thus contributed more to runoff and drainage (Fig. 7c) than to transpiration (Fig. 7b) and productivity, as has been observed experimentally (Chou et al., 2008). Annual NEP was also not well correlated with the length of the growing season determined by dates of green-up and senescence (modelled: $R^2 = 0.11$, $P < 0.4$; EC: $R^2 = 0.25$, $P < 0.2$). This correlation was reduced by an apparently long growing season with low NEP in 2008 caused by the irregular start to the rainy season in autumn 2007 (Fig. 1s) which delayed net C uptake (Fig. 1x). Annual NEP was better correlated with the duration of net C uptake determined by the dates on which continuous net C uptake began and ended (modelled: $R^2 = 0.82$, $P < 0.01$; EC: $R^2 = 0.53$, $P < 0.05$ in Table 4).

In the model, the duration of net C uptake was determined by the timing of germination and senescence when requirements had been met for hours accumulated at ψ_c above or below set thresholds respectively, or when physiological maturity was reached. These requirements enabled the modelled plants to avoid premature germination and consequent depletion of seed stocks with false starts to the rainy season (e.g. during August 2003 in Fig. 1g), and premature senescence and consequent loss of seed production with false ends to the rainy season (e.g. March 2004 in Fig. 1j). These requirements also enabled the modelled plants to make optimal use of soil water for plant growth and seed production during the rainy season while minimizing losses of remobilizable C to litterfall with senescence at the end of the rainy season. In conjunction with the set timing of vegetative and reproductive growth stages between germination and senescence, these requirements enabled sustained growth by annual plants dependent on seed germination to be modelled under a highly variable climate (e.g. Fig. 8a).

The duration of net C uptake in the model was found not to be very sensitive to the values of the time requirements and ψ_c thresholds for germination and senescence because the time requirements were sufficient to distinguish false from real changes in season, and when these changes occurred, ψ_c alternated between values much higher or lower than the thresholds. Therefore the time requirements and ψ_c thresholds proposed here meet the requirements of the first algorithm in the Introduction for representing the climatic signals that initiate and terminate C uptake by annual plants in Mediterranean climates. However other schemes for identifying changes in water status could also be used to model the timing of net C uptake in seasonally dry ecosystems (e.g. Botta et al., 2000; Jolly and Running, 2004). The biological basis of signals for germination and senescence in drought-adapted annual ecosystems needs further clarification.

Values of ψ_c modelled during net C uptake were determined from coupled equations for equilibrating root water uptake and canopy transpiration in the model [B14]. These values gave r_c [B3, C4] that allowed changes in *LE* [B1] and net CO_2 uptake [C2, C6, C7] to be accurately modelled on dry *vs*. wet soils (e.g. Fig. 3h, i *vs*. k, l), as found in earlier studies (e.g. Grant and Flanagan, 2007; Grant et al., 2009). These coupled equations therefore continue to meet requirements of the second algorithm in the Introduction for modelling the effects of soil and atmospheric water status on gross primary productivity (GPP) and hence on plant C uptake during soil wetting and drying.

Net C uptake modelled and measured during the later rainy season was largely offset by net C emissions modelled and measured from rewetted surface residue and soil following rainfall events during the first two to three months of the rainy season (Fig. 1). Modelling the rapid onset and decline of net C emissions observed with wetting and drying after these events (Chou et al., 2008; Xu and Baldocchi, 2004) was therefore necessary to modelling annual NEP. This was achieved (Fig. 2) with coupled equations for decomposition [A3, A4] and microbial respiration [A13] based on values of [*M*] that were highly sensitive to changes in residue and soil θ. These same equations have been used to model the time course of soil respiration following residue amendments at different ψ_s in controlled incubations (Grant and Rochette, 1994), and so appear to be robust. These equations therefore meet the requirements of the third algorithm in the Introduction for modelling the effects of soil wetting and drying on R_h.

4.2. Net ecosystem productivity under climate change

These algorithms raised annual modelled NEP in years with shorter rainy seasons and lowered it in years with longer rainy seasons during climate change under SRES A1fi and B1 emission scenarios from HadCM3 (Fig. 6). In years with shorter rainy seasons, rates of net C uptake rose with C_a and T_a while the duration of net C uptake was not affected, thereby raising NEP. This model result was based on the assumption that lengths of rainy seasons during climate change will not differ from those under current climate. This assumption was a consequence of applying changes in monthly mean T_a and precipitation predicted by HadCM3 (Table 2) to hourly values recorded under current climate. The application of these changes allowed diurnal and interannual variation in current weather to be maintained during climate change. This variation strongly affects ecosystem processes, and so the application of these changes to historical weather data has been widely used in studies of climate change impacts on ecosystem function (e.g. Hayhoe et al., 2004). Such application effectively removed any bias of mean GCM climatology from the projected climate, but it could constrain interannual variability in climate projections to that in current climates (Vicuna et al., 2007). Interannual variability in rainy seasons simulated for California during the 21st century under different climate change scenarios has not differed much from that simulated under historical climate (Cayan et al., 2008), supporting the validity of this assumption. However Giorgi (2006) estimated that interannual variability of precipitation in Mediterranean regions could rise with climate change, so that alternative precipitation scenarios might be included in future projections.

In years with longer rainy seasons, rates of net C uptake also rose with C_a and T_a, but the duration of net C uptake declined with warming due to hastened plant maturity. Consequently peak plant biomass rose little with climate change, as found experimentally for California grasslands by Dukes et al. (2005). Earlier plant maturity left wet soil with rapid C emissions from R_h under high θ and T_s at the end of the rainy season (Fig. 6). Experimental warming has been observed to hasten flowering and reproductive growth of annual tallgrass prairie species (Sherry et al., 2007), and to hasten senescence of annual grassland species in Mediterranean climate zones (Zavaleta et al., 2003). Earlier senescence with warming has been found to leave wetter soil at the end of the rainy season, indicating phenology-driven declines in water use (Zavaleta et al., 2003). As climate change progressed in the model, this earlier senescence caused a growing mismatch between the duration of annual grassland life cycles and that of rainy seasons. This mismatch caused greater net C emissions to be modelled at the end of rainy seasons than those modelled and measured under current climate (Fig. 6 *vs*. Fig. 1o), thereby lowering annual NEP. These emissions also drove more rapid N mineralization that increased NPP and hence NEP the following year. These increased emissions in the model were consistent with experimental findings that late season rainfall did not extend net C uptake but did increase net C emissions by 20–30 $\mathrm{g\,C\,m^{-2}}$ from annual grasslands in Mediterranean climate zones (Chou et al., 2008). The increased C emissions modelled under climate change were based on an assumption of no change in species diversity or phenological adaptation in a warmer climate. These modelled and experimental results indicate the importance of understanding climate change effects on phenology as well as on CO_2 exchange in studies of climate change impacts on ecosystem productivity, especially of those dominated by annual plant species.

As climate change progressed in the model, rises in net C emission from warmer, wetter soil gradually exceeded rises in net C uptake from higher C_a and T_a (Fig. 8a), causing annual NEP to decline with an eventual loss of ecosystem sink activity (Fig. 8b, c). Rises in net C uptake modelled during climate change were slowed by declining N_2 fixation in declining legume populations caused by increasing grass productivity under rising C_a and T_a, attributed in the model to more rapid N uptake from warmer, more rapidly mineralizing soils. This model result was consistent with observations by Pitt and Heady (1978) that legume composition in California annual grasslands can decline to as low as 2% from more rapid grass growth on soils with improved N fertility. This model result may have been an artifact of the biological properties with which the annual grass and legume PFTs were initialized, but may indicate that climate change effects on ecosystem productivity may be mediated in part by changes in plant community composition. The declines in NEP with climate change modelled here were consistent with those modelled under a range of climate change scenarios by Morales et al. (2007), in which European Mediterranean ecosystems became greater C sources after 110 years. Collectively, these model results indicate that climate change will likely have adverse effects on NEP of annual grassland ecosystems in Mediterranean climate zones at some time in the future, depending on the rate or climate warming, unless there is selection for longer life cycles in annual plant species, or replacement of annual species by perennial ones.

Acknowledgements

Computing facilities for *ecosys* were provided by the University of Alberta and by Cybera, a corporation managing cyberinfrastructure-related technologies in collaboration with academic and industry partners. The field research was supported in part by the Office of Science (BER), U.S. Department of Energy, Grant No. DE-FG02-03ER63638 and through the Western Regional Center of the National Institute for Global Environmental Change under Cooperative Agreement No. DE-FC02-03ER63613. Other sources of support included the Kearney Soil Science Foundation, the National Science Foundation and the Californian Agricultural Experiment Station.

Appendix A. Supplementary data

Supplementary data associated with this article can be found, in the online version, at doi:10.1016/j.agrformet.2011.09.012.

References

Baldocchi, D.D., Xu, L., Kiang, N., 2004. How plant functional-type, weather, seasonal drought, and soil physical properties alter water and energy fluxes of an oak–grass savanna and an annual grassland. Agric. For. Meteorol. 123, 13–39.

Botta, A., Viovy, N., Ciais, P., Friedlingsein, P., Monfray, P., 2000. A global prognostic scheme of leaf onset using satellite data. Global Change Biol. 6, 709–725.

Cayan, D.R., Maurer, E.P., Dettinger, M.D., Tyree, M., Hayhoe, K., 2008. Climate change scenarios for the California region. Climatic Change 87, S21–S42.

Christensen, J.H., Hewitson, B., Busuioc, A., Chen, A., Gao, X., Held, I., Jones, R., Kolli, R.K., Kwon, W.-T., Laprise, R., Magaña Rueda, V., Mearns, L., Menéndez, C.G., Räisänen, J., Rinke, A., Sarr, A., Whetton, P., 2007. Regional climate projections. In: Solomon, S., Qin, D., Manning, M., Chen, Z., Marquis, M., Averyt, K.B., Tignor, M., Miller, H.L. (Eds.), Climate Change 2007: The Physical Science Basis. Contribution of Working Group I to the Fourth Assessment Report of the Intergovernmental Panel on Climate Change. Cambridge University Press, Cambridge, United Kingdom and New York, NY, USA.

Chou, W.W., Silver, W.L., Jackson, R.D., Thompson, A.W., Allen-Diaz, B., 2008. The sensitivity of annual grassland carbon cycling to the quantity and timing of rainfall. Global Change Biol. 14 (6), 1382–1394.

Dukes, J.S., Chiariello, N.R., Cleland, E.E., Moore, L.A., Shaw, M.R., Thayer, S., Tobeck, T., Mooney, H.A., Field, C.B., 2005. Responses of grassland production to single and multiple global environmental changes. PLoS Biol. 3, 1829–1837.

Giorgi, F., 2006. Climate change hot-spots. Geophys. Res. Lett. 33, L08707, doi:10.1029/2006GL025734.

Grant, R.F., 1989. Simulation of maize phenology. Agron. J. 81, 451–457.

Grant, R.F., 1998. Simulation in *ecosys* of root growth response to contrasting soil water and nitrogen. Ecol. Model. 107, 237–264.

Grant, R.F., Juma, N.G., McGill, W.B., 1993a. Simulation of carbon and nitrogen transformations in soils. I. Mineralization. Soil Biol. Biochem. 27, 1317–1329.

Grant, R.F., Juma, N.G., McGill, W.B., 1993b. Simulation of carbon and nitrogen transformations in soils. II. Microbial biomass and metabolic products. Soil Biol. Biochem. 27, 1331–1338.

Grant, R.F., Rochette, P., 1994. Soil microbial respiration at different temperatures and water potentials: theory and mathematical modelling. Soil Sci. Soc. Am. J. 58, 1681–1690.

Grant, R.F., Wall, G.W., Frumau, K.F.A., Pinter Jr., P.J., Hunsaker, D., Kimball, B.A., LaMorte, R.L., 1999. Crop water relations under different CO_2 and irrigation: testing of *ecosys* with the Free Air CO_2 Enrichment (FACE) Experiment. Agric. For. Meteorol. 95, 27–51.

Grant, R.F., Flanagan, L.B., 2007. Modeling stomatal and nonstomatal effects of water deficits on CO_2 fixation in a semiarid grassland. J. Geophys. Res. 112, G03011, doi:10.1029/2006JG000302.

Grant, R.F., Barr, A.G., Black, T.A., Margolis, H.A., Dunn, A.L., Metsaranta, J., Wang, S., McCaughey, J.H., Bourque, C.P.-A., 2009. Interannual variation in net ecosystem productivity of Canadian forests as affected by regional weather patterns – a Fluxnet-Canada synthesis. Agric. For. Meteorol. 149, 2022–2039.

Grant, R.F., Arkebauer, T.J., Dobermann, A., Hubbard, K.G., Schimelfenig, T.T., Suyker, A.E., Verma, S.B., Walters, D.T., 2007a. Net biome productivity of irrigated and rainfed maize–soybean rotations: modelling vs. measurements. Agron. J. 99, 1404–1423.

Grant, R.F., Barr, A.G., Black, T.A., Iwashita, I., Kidson, J., McCaughey, H., Morgenstern, K., Murayama, S., Nesic, Z., Saigusa, N., Shashkov, A., Zha, T., 2007b. Net ecosystem productivity of boreal jack pine stands regenerating from clearcutting under current and future climates. Global Change Biol. 13, 1423–1440.

Grant, R.F., Black, T.A., Humphreys, E.R., Morgenstern, K., 2007c. Changes in net ecosystem productivity with forest age following clearcutting of a coastal Douglas fir forest: testing a mathematical model with eddy covariance measurements along a forest chronosequence. Tree Physiol. 27, 115–131.

Grant, R.F., Margolis, H.A., Barr, A.G., Black, T.A., Dunn, A.L., Bernier, P.Y., Bergeron, O., 2008. Changes in net ecosystem productivity of boreal black spruce stands in response to changes in temperature at diurnal and seasonal time scales. Tree Physiol. 29, 1–17.

Grant, R.F., Black, T.A., Gaumont-Guay, D., Kljun, N., Barr, A.G., Morgenstern, K., Nesic, Z., 2006. Net ecosystem productivity of boreal aspen forests under drought and climate change: mathematical modelling with *ecosys*. *FCRN Special Issue*. Agric. For. Meteorol. 140, 152–170.

Grant, R.F., Kimball, B.A., Conley, M.M., White, J.W., Wall, G.W., Ottman, M.J., 2011. Controlled warming effects on wheat growth and yield: field measurements and modeling. Agron. J. 103, 1742–1754.

Hayhoe, K., Cayan, D.R., Field, C.B., Frumhoff, P.C., Maurer, E., Miller, N., Moser, S., Schneider, S., Cahill, K., Cleland, E., Dale, L., Drapek, R., Hanemann, R.M., Kalkstein, L., Lenihan, J., Lunch, C., Neilson, R., Sheridan, S., Verville, J., 2004. Emissions pathways, climate change, and impacts on California. Proc. Natl. Acad. Sci. (PNAS) 101 (34), 12422–12427.

Huntsinger, L., Bartolome, J.W., D'Antonio, C., 2007. Grazing management on California's Mediterranean Grasslands. In: Stromberg, M., Corbin, J., D'Antonio C (Eds.), California Grasslands: Ecology and Management. University of California Press, Berkeley, pp. 233–253.

Huxman, T.E., Snyder, K.A., Tissue, D., Leffler, A.J., Ogle, K., Pockman, W.T., Sandquist, D.R., Potts, D.L., Schwinning, S., 2004. Precipitation pulses and carbon fluxes in semiarid and arid ecosystems. Oecologia 141, 254–268.

Jolly, W.M., Running, S.W., 2004. Effects of precipitation and soil water potential on drought deciduous phenology in the Kalahari. Global Change Biol. 10, 303–308.

Lindner, M., Maroschek, M., Netherer, S., Kremer, A., Barbati, A., Garcia-Gonzalo, J., Seidl, R., Delzon, S., Corona, P., Kolström, M., Lexer, M.J., Marchetti, M., 2010. Climate change impacts, adaptive capacity, and vulnerability of European forest ecosystems. Forest Ecol. Manage. 259, 698–709.

Ma, S., Baldocchi, D.D., Xu, L., Hehn, T., 2007. Inter-annual variability in carbon dioxide exchange of an oak/grass savanna and open grassland in California. Agric. For. Meteorol. 147, 157–171.

Meehl, G.A., Stocker, T.F., Collins, W.D., Friedlingstein, P., Gaye, A.T., Gregory, J.M., Kitoh, A., Knutti, R., Murphy, J.M., Noda, A., Raper, S.C.B., Watterson, I.G., Weaver, A.J., Zhao, Z.-C., 2007. Global climate projections. In: Solomon, S., Qin, D., Manning, M., Chen, Z., Marquis, M., Averyt, K.B., Tignor, M., Miller, H.L. (Eds.), Climate Change 2007: The Physical Science Basis. Contribution of Working Group I to the Fourth Assessment Report of the Intergovernmental Panel on Climate Change. Cambridge University Press, Cambridge, United Kingdom and New York, NY, USA.

Morales, P., Hickler, T., Rowell, D.P., Smith, B., Sykes, M.T., 2007. Changes in European ecosystem productivity and carbon balance driven by regional climate model output. Global Change Biol. 13, 108–122.

Pereira, J.S., Mateus, J.A., Aires, L.M., Pita, G., Pio, C., David, J.S., Andrade, V., Banza, J., David, T.S., Paço, T.A., Rodrigues, A., 2007. Net ecosystem carbon exchange in three contrasting Mediterranean ecosystems – the effect of drought. Biogeosciences 4, 791–802.

Pitt, M.D., Heady, H.F., 1978. Responses of annual vegetation to temperature and rainfall patterns in northern California. Ecology 59, 336–350.

Richardson, A.D., Hollinger, D.Y., Burba, G.G., Davis, K.J., Flanagan, L.B., Katul, G.G., Munger, J.W., Ricciuto, D.M., Stoy, P.C., Suyker, A.E., Verma, S.B., Wofsy, S.C., 2006. A multi-site analysis of random error in tower-based measurements of carbon and energy fluxes. Agric. For. Meteorol. 136, 1–18.

Rutledge, S., Campbell, D.I., Baldocchi, D., Schipper, L.A., 2010. Photodegradation leads to increased carbon dioxide losses from terrestrial organic matter. Global Change Biol., doi:10.1111/j.1365-2486.2009.02149.x.

Saxton, K.E., Rawls, W.J., Romberger, J.S., Papendick, R.I., 1986. Estimating generalized soil-water characteristics from texture. Soil Sci. Soc. Amer. J. 50, 1031–1036.

Sherry, R.A., Zhou, X., Gu, S., Arnone, J.A., Schimel, D.S., Verburg, P.S., Wallace, L.L., Luo, Y., 2007. Divergence of reproductive phenology under climate warming. PNAS 104, 198–202.

Vicuna, S., Maurer, E.P., Joyce, B., Dracup, J.A., Purkey, D., 2007. The sensitivity of California water resources to climate change scenarios. J. Am. Water Resour. Assoc. 43 (2), 482–498.

Wesely, M.L., Hart, R.L., 1985. Variability of short term eddy-correlation estimates of mass exchange. In: Hutchinson, B.A., Hicks, B.B. (Eds.), The Forest–Atmosphere Interaction. D. Reidel, Dordrecht, pp. 591–612.

Xu, L., Baldocchi, D.D., 2004. Seasonal variation in carbon dioxide exchange over a Mediterranean annual grassland in California. Agric. For. Meteorol. 1232, 79–96.

Zavaleta, E.S., Thomas, B.D., Chiariello, N.R., Asner, G.P., Shaw, M.R., Field, C.B., 2003. Plants reverse warming effect on ecosystem water balance. PNAS 100, 9892–9893.